Clim. Past Discuss., 7, 3583–3607, 2011
www.clim-past-discuss.net/7/3583/2011/
doi:10.5194/cpd-7-3583-2011

Climate
of the Past
Discussions

Title Page
Abstract | Introduction
Conclusions | References
Tables | Figures
◀| | |▶
◀ | ▶
Back | Close
Full Screen / Esc
Printer-friendly Version
Interactive Discussion

A model comparison study for the Antarctic region: present and past

M. N. A. Maris, B. de Boer, and J. Oerlemans

Institute for Marine and Atmospheric research Utrecht, Utrecht University, P.O. Box 80005,
3508 TA Utrecht, The Netherlands

Received: 7 October 2011 – Accepted: 12 October 2011 – Published: 24 October 2011

Correspondence to: M. N. A. Maris (m.n.a.maris@gmail.com)

Published by Copernicus Publications on behalf of the European Geosciences Union.

Abstract

Eighteen global climate models (GCMs) are compared to reference data for the present, the mid-Holocene (MH) and the last glacial maximum (LGM) for the Antarctic region. For the present, the reference data come from a regional climate model. GCM results for the past are compared to ice core data. The goal of this study is to find the best GCM to model the evolution of the Antarctic Ice Sheet. Because temperature and precipitation are the most important climate variables when modelling the evolution of an ice sheet, these two variables are considered in this paper. In general, present-day temperature is simulated well, but precipitation is overestimated compared to the reference state. Some other findings are that the air above ice shelves is too warm and precipitation in the coastal region of the western peninsula is underestimated by the models, as compared to the present-day reference state. Furthermore, model biases play an important role in simulating the past, as they are often larger than the change in temperature or precipitation between the past and the present. Considering the results for the present-day as well as for the MH and the LGM, the best performing models are HadCM3 and MIROC 3.2.2.

1 Introduction

Variations in ice volume of the Antarctic Ice Sheet (AIS) have a large impact on sea level and ocean circulation. Since the last glacial maximum (LGM), at approximately 21 ka, the AIS has undergone many changes (e.g. Huybrechts, 2002; Pollard and DeConto, 2009). This is especially true for the West Antarctic Ice Sheet, which is potentially unstable (see for example, Hughes, 1975; Thomas, 1979; Bamber et al., 2009). To study variations in the AIS with a dynamical ice sheet model, realistic (near-surface) air temperature and precipitation are needed as input. These variables may be given by a global climate model (GCM), therefore it is important to know which GCMs perform well.

The Paleoclimate Modelling Intercomparison Project Phase II (PMIP2; Braconnot et al., 2007) has a large database with output from GCMs, for the present, the mid-Holocene (MH) and the LGM. Some earlier intercomparison studies of the models in this database have been done by, amongst others, Braconnot et al. (2007), Yanase and Abe-Ouchi (2007), Brewer et al. (2007) and Masson-Delmotte et al. (2006). Only the study of Masson-Delmotte et al. (2006) focuses on the polar regions and therefore also includes Antarctica. They conclude that the PMIP2 models' simulations agree reasonably well with ice core signals for both the MH and the LGM, although there are uncertainties in the models' ice sheet topography, which is based on ICE-5G (Peltier, 2004).

In former studies, little attention has been paid to the individual model performance and differences between models. In order to decide which GCMs perform best in the Antarctic region we compare the individual models' output to ice core observations for the MH and LGM in this paper. Furthermore, as ice core data have a large uncertainty and do not cover the entire Antarctic region, we compare present-day GCM data to a reference state from RACMO2/ANT (Lenaerts et al., 2010). RACMO2/ANT (simply "RACMO" hereafter) is a regional climate model, developed especially for polar regions and thoroughly validated (e.g. van de Berg et al., 2005; Lenaerts et al., 2010).

2 Method

Eighteen models from the PMIP2 database, see Table 1, are compared with reference data from RACMO. The GCM-data used for this study come from coupled ocean-atmosphere (oa) models. For some models there are also data available from an ocean-atmosphere-vegetation (oav) version, but the difference in output between the oa- and oav-versions is negligible for Antarctica. Some of the models are closely related to others: CSIRO-1.1 is the same as CSIRO-1.0, but with a doubled oceanic resolution; MRI-fa uses flux adjustments for heat and water fluxes and wind stress, whereas MRI-nfa does not; and MIROC 3.2.2 is the same as MIROC 3.2, but an error in the land surface scheme of MIROC 3.2 has been corrected in MIROC 3.2.2, affecting the wind stress calculation over ice sheets and resulting in somewhat lower temperatures.

The reference state comes from RACMO, which is run with lateral boundaries of the ERA-Interim reanalysis, for 20 years (1989–2009), and with a horizontal resolution of 27 km. The domain runs from 90° S to approximately 47° S. We compared 2m air temperature and annual mean precipitation with RACMO-data, interpolated on the corresponding GCM-grid. The data are compared regarding correlation coefficient, bias and root mean square deviation (rmsd). The correlation coefficient indicates how well temperature and precipitation patterns are represented by a model, whereas the bias (mean deviation of the model from the reference) and the rmsd (a measure for the absolute deviation of the model from the reference) quantify how much the model output deviates from the reference state as a whole. A distinction is made between results over the entire domain (Fig. 1) and solely over the ice sheet, including ice shelves (Fig. 2).

In the second part of this study, GCM output for the MH (6 ka) and the LGM (21 ka) is compared to the present. Differences between the past and the present are evaluated, using observations from ice cores. Temperature data are available from six ice cores for both the MH and the LGM: EPICA Dome C (EDC) (Jouzel and Masson-Delmotte, 2007), EPICA Dronning Maud Land (Stenni et al., 2010), Dome Fuji (Kawamura et al., 2007), Law Dome (van Ommen et al., 2004), Taylor Dome (Steig et al., 2000) and Vostok (Petit et al., 1999), except for Taylor Dome, which misses data for the MH. Precipitation records are scarce as they are hard to derive from ice cores. The data used for comparison here are from Law Dome (van Ommen et al., 2004), Talos Dome (Buiron et al., 2011) and Vostok (Steig et al., 2000).

Model results are compared with ice core data with respect to temperature difference between the past and the present, precipitation difference between the past and the present and the ratio of past to present precipitation. This is because some models, for example, give a correct change in precipitation, but overestimate the actual amount both in the past and for the present-day. In this case the modelled ratio will be larger than the ratio deduced from the ice core. The comparison is realized by interpolating the data from the four grid points of the GCM closest to the location of the ice core.

3 Present-day results

Figure 1 shows the bias (in blue) and the rmsd (in red) for the present-day comparison between the PMIP2-models and RACMO over the entire RACMO-domain. The biases range from −4.5 K (FOAM) to +2.7 K (GISS) and the rmsd values go up to 7.7 K (Ecbiltclio) for the temperature. Temperature correlation coefficients (not shown) are close to 1, ranging from 0.93 to 0.99, for all models. This is due to the dominant relation between temperature and altitude over land, and the strong latitude dependence of temperature over the ocean. Precipitation biases are dominantly positive. The highest value is +470 mm yr^{-1} for ECHAM5, which also shows the highest rmsd value of 666 mm yr^{-1}. ECHAM53 is a newer version of this model and clearly performs much better regarding both temperature and precipitation over the Antarctic. Precipitation correlation coefficients show a larger spread than for temperature, from 0.78 to 0.90. The most extreme bias and rmsd come from ECHAM5 for precipitation data, resulting from a strong overestimation of the precipitation over the ocean and from FOAM for temperature data, which might be due to the low resolution of the model. As mentioned before, the model MIROC 3.2.2 should give lower temperatures than MIROC 3.2 due to a corrected error in the latter, which is indeed the case.

In Fig. 2 the same variables are presented as in Fig. 1, but for a domain that only incorporates ice covered grid points. Again, the temperature correlation coefficients are close to 1, ranging from 0.91 to 0.97, except for Ecbiltclio (0.49) and Ecbiltcliovecode (0.53), but smaller than for the entire domain. This is due to the strong latitude dependence of temperature over the ocean, which is well represented by all models, whereas the temperature patterns over the ice sheet are less well simulated. Precipitation correlation coefficients show a large spread for this smaller domain and are generally lower (from 0.62 to 0.88), while bias and rmsd values are also lower. This is often the result of an overestimation or underestimation of precipitation over the ocean and is especially true for ECHAM5, which strongly overestimates the precipitation over the ocean, but performs much better over the ice sheet.

More detailed results are shown in Fig. 3, which presents the temperature difference fields between four of the GCMs and RACMO for the present-day. In CNRM the air over the ice shelves is too warm by as much as 20 K, probably caused by modelling sea ice instead of ice shelves. This feature is present in other models as well. For FGOALS the bias in temperature is low, but the air over the ocean is too cold and over the ice sheet too warm, so the rmsd is high. These inverse temperature biases over land and over water are also seen in other GCMs. As has been concluded from Fig. 1, FOAM has the coldest bias, which mainly comes from too low temperatures over the ocean, see Fig. 3c. MIROC 3.2.2 is also shown in this figure because it gives the best results for temperature.

Precipitation difference fields are presented in Fig. 4 for two GCMs. ECHAM5 strongly overestimates the precipitation over the ocean, as has been noted earlier. However, the precipitation over the ice sheet has been modelled more accurately. MIROC 3.2.2 is one of the best performing models and therefore shown as well. The plot also shows an interesting feature, present in all models, namely a negative bias in precipitation on the Bellingshausen Sea and Amundsen Sea coasts. This local bias decreases slightly with higher model resolution.

4 Mid-Holocene results

Mid-Holocene results from the models are compared to five ice cores in Table 2. Temperature differences with the present are small and mostly overestimated by the models, especially by MRI-fa, which gives very high temperatures over the entire domain at 6 ka. This might be a timing problem, as the Antarctic climate optimum ended just before 6 ka (Ciais et al., 1992).

To point out some interesting spatial patterns, Fig. 5 presents the temperature difference fields between 6 ka and the present for two GCMs. FGOALS shows higher temperatures at 6 ka than at the present in the same band that is modelled too cold in the present, as compared to RACMO (see Fig. 5b). The same feature is seen in the data from CCSM. Near the coast, temperature differences are modelled somewhat less positive than observed in the EDML and Law Dome ice cores (sqares in Fig. 5b), see Table 2. However, according to the ice core data from EDC and Fuji (stars in Fig. 5b) the modeled temperature differences are too positive further inland. This pattern is the inverse of the difference between present-day CCSM-data and RACMO (not shown) where the air is too cold over the inland and too warm over the coasts. These two examples show an overestimation of temperature differences where there is a cold present-day bias and vice versa. This compensational behaviour might lead to more realistic temperatures at 6 ka.

In Table 3 precipitation data are shown for three ice core locations. The Law Dome data are not very accurate as only the average accumulation between age ties (2545 and 6778 years ago) is known, but ECHAM5 probably underestimates the amount of precipitation at 6 ka, as it also does at the Talos Dome and Vostok locations. The large deviation of ECHAM5 from the other models and the ice core observations is probably caused by the strong overestimation of present-day precipitation (see Fig. 4a). At the Talos Dome location, the amount of precipitation is overestimated by all models, although some capture the difference in precipitation between 6 ka and the present. Most of the GCMs simulate precipitation at the Vostok location quite accurately, which might have to do with its more inland position.

When examining model results for the past, present-day biases play a role, as noted before for CCSM and FGOALS specifically. To investigate that role a signal-to-noise ratio has been calculated for both temperature and precipitation. The signal is the difference, in temperature or precipitation, between 6 ka and the present. The noise is the present-day bias of a model, as shown in Fig. 1. For precipitation the average signal-to-noise ratio of all GCMs is 0.04, which means that the signal is practically nondeductible from the data. The mean signal-to-noise ratio for temperature is 0.14. Consequently, present performance of a model should be taken into account when analysing data for 6 ka to differentiate between patterns due to bias and the real signal.

5 LGM results

In Table 4 modelled temperature differences between the LGM and the present are compared to data from six ice cores. At Law Dome and Taylor Dome temperature differences are the smallest, which is only partly captured by CNRM and HadCM3. There are two possible reasons for this: Firstly, the models might not be capable of simulating the differences between coastal and inland temperature evolution well enough. Secondly, coastal ice cores are more challenging to interpret (Buiron et al., 2011), so the observed temperature change has a larger uncertainty at Law Dome and Taylor Dome.

FGOALS overestimates the temperature differences at all six locations, whereas CNRM underestimates all temperature differences. This is also illustrated in Fig. 6, where the temperature difference fields between 21 ka and the present are shown for these two GCMs. A band of smaller (i.e. less negative) temperature differences is visible in the FGOALS-data at the same location as the warm band at 6 ka, see Sect. 4. LGM temperatures over the ocean are probably overestimated by CNRM as they are even higher at the LGM than at the present and were already overestimated in the present, compared to RACMO.

Modelled precipitation differences between the LGM and the present are compared to Law Dome, Talos Dome and Vostok data in Table 5. For Law Dome the LGM-precipitation was less than 10 % of the present-day value. Including other estimates, the LGM precipitation ranges from 5 to 10 % of the present value at this site. Data from Taylor Dome also show a small amount of LGM precipitation, namely less than 20 % of its present value. The Law Dome and Taylor Dome ice cores are both located near the coast, where they receive precipitation from cyclonic systems. These systems have probably changed since the LGM, causing a large change in precipitation in coastal regions (van Ommen et al., 2004). None of the models have captured this change, as the cyclonic systems are presumably too small to simulate correctly.

Figure 7 shows some more detailed precipitation differences between the LGM and the present for CNRM and MIROC 3.2.2. CNRM shows speckled results, which is also the case for the difference between its present-day precipitation data and RACMO. This indicates a problem with modelling precipitation specifically, as the speckles are not present in the temperature results. One of the best performing models is MIROC 3.2.2, for which the difference field is shown in Fig. 7b. Overall the LGM was drier than the present, while the tip of the peninsula is modelled to have been wetter. This is true for most of the models and might be connected to the underestimation of western peninsula precipitation at 0 ka. However, as there is no evidence to the contrary the models' results cannot be negated.

As for the MH, the signal-to-noise ratio has been calculated for the LGM as well, to study the influence of the models' biases on the simulation of precipitation and temperature patterns at 21 ka. The average signal-to-noise ratio for temperature is 4.8, meaning that the signal of temperature change from the LGM to the present is discernible when studying the model output. For precipitation the mean signal-to-noise ratio is 0.41. The main reason for this low number is the high bias (the noise) of FGOALS, see also Fig. 1. Although these ratios are higher than for the MH, it is still essential to be aware of the (present-day) bias of a model to correctly assess its output for the LGM.

6 Conclusions

In this paper we compared present-day output from GCMs in the PMIP2 project to a reference state from the regional climate model RACMO2/ANT for the Antarctic region. We found that air temperature patterns are generally well modelled, although temperature is more correctly simulated over the ocean than over the ice sheet. The temperature over the ice shelves is too high in most of the models, which is probably because ice shelves are not simulated, so the air over the ocean only cools in winter when there is sea ice. Furthermore, we noted that in most of the models the temperature bias over the ice sheet is the inverse of the temperature bias over the ocean. This may be the result of the closed energy balance in these models. In other words, if the temperature is overestimated over land, a compensation is made over the water, leading to an underestimation of temperature there and vice versa.

Precipitation patterns are also well modelled in general, but the actual amount of precipitation over the ice sheet is overestimated by all models and often strongly over- or underestimated over the ocean. In addition, a negative bias was observed over the Bellingshausen and Amundsen Sea coasts. The models probably do not resolve the circulation pattern well enough to simulate the additional precipitation in this region (Rojas et al., 2009). Considering all results for the present-day, the four models that perform best are ECHAM53, HadCM3, MIROC 3.2.2 and UBRIS.

Patterns in present-day output are very important for a model's performance at the MH and LGM. For instance, in some models we noticed an overestimation of the temperature difference between the MH and the present, where there was a cold bias in the present and vice versa. The importance of present-day results is also clear from the signal-to-noise ratios we found for the MH (0.04 for precipitation and 0.14 for temperature) and for the LGM (0.41 for precipitation and 4.8 for temperature).

The low signal-to-noise ratios indicate large uncertainties in the models' data, but there are two other sources of uncertainties in the comparison between model results and ice core observations. The first source is the ice core; temperature and precipitation in the past are not measured with 100 % certainty, nor is the timing known with such precision. The second source is the elevation. As Masson-Delmotte et al. (2006) state in their paper, there might be a discrepancy between the elevation at which the surface was in the past and the elevation that is modelled. However, the past elevation of the ice sheet is not known with great accuracy, nor is the lapse rate, so we decided not to correct for this discrepancy.

To conclude, although signal-to-noise ratios are low and uncertainties in ice core data and past elevation are quite large, some models simulate temperature and precipitation differences between the past and the present quite well. Not all models provided data for the MH or the LGM, but, among the models that did provide data, the best performing models for 6 ka are MIROC 3.2, FGOALS and CSIRO-1.0. For 21 ka HadCM3 and MIROC 3.2.2 achieved the best results. Finally, considering both present-day and past simulations, the best performing models according to our comparison, in simulating temperature and precipitation in the Antarctic region, are HadCM3 and MIROC 3.2.2.

Acknowledgements. We acknowledge the international modelling groups for providing their data for analysis and the Laboratoire des Sciences du Climat et de l'Environnement (LSCE) for collecting and archiving the model data. The PMIP2 Data Archive is supported by CEA, CNRS and the Programme National d'Etude de la Dynamique du Climat (PNEDC). The analyses were performed using version 03-01-2011 of the database. More information is available on http://pmip2.lsce.ipsl.fr/. Additionally, we would like to thank J. Lenaerts for providing us with data from RACMO2/ANT.

References

Bamber, J., Riva, R., Vermeersen, B., and LeBrocq, A.: Reassessment of the potential sea-level rise from a collapse of the WAIS, Science, 324, 901–903, doi:10.1126/science.1169335, 2009. 3584

Braconnot, P., Otto-Bliesner, B., Harrison, S., Joussaume, S., Peterchmitt, J.-Y., Abe-Ouchi, A., Crucifix, M., Driesschaert, E., Fichefet, Th., Hewitt, C. D., Kageyama, M., Kitoh, A., Laîné, A., Loutre, M.-F., Marti, O., Merkel, U., Ramstein, G., Valdes, P., Weber, S. L., Yu, Y., and Zhao, Y.: Results of PMIP2 coupled simulations of the Mid-Holocene and Last Glacial Maximum - Part 1: experiments and large-scale features, Clim. Past, 3, 261–277, doi:10.5194/cp-3-261-2007, 2007. 3585

Brewer, S., Guiot, J., and Torre, F.: Mid-Holocene climate change in Europe: a data-model comparison, Clim. Past, 3, 499–512, doi:10.5194/cp-3-499-2007, 2007. 3585

Buiron, D., Chappellaz, J., Stenni, B., Frezzotti, M., Baumgartner, M., Capron, E., Landais, A., Lemieux-Dudon, B., Masson-Delmotte, V., Montagnat, M., Parrenin, F., and Schilt, A.: TALDICE-1 age scale of the Talos Dome deep ice core, East Antarctica, Clim. Past, 7, 1–16, doi:10.5194/cp-7-1-2011, 2011. 3586, 3590

Ciais, P., Petit, J., Jouzel, J., Lorius, C., Barkov, N., Lipenkov, V., and Nicolaïev, V.: Evidence for an early Holocene climatic optimum in the Antarctic deep ice-core record, Clim. Dynam., 6, 169–177, 1992. 3588

Hughes, T.: The West Antarctic Ice Sheet: Instability, disintegration, and initiation of Ice Ages, Rev. Geophys. Space Phys., 13, 502–526, 1975. 3584

Huybrechts, P.: Sea-level changes at the LGM from ice-dynamic reconstructions of the Greenland and Antarctic ice sheets during the glacial cycles, Quaternary Sci. Rev., 21, 203–231, 2002. 3584

Jouzel, J. and Masson-Delmotte, V.: EPICA Dome C ice core 800kyr deuterium data and temperature estimates, IGBP PAGES/World Data Center for Paleoclimatology data contribution series 2007-091, NOAA/NCDC Paleoclimatology Program, Boulder CO, USA, 2007. 3586

Kawamura, K., Uemura, R., Hideaki, M., Fujita, S., Azuma, K., Fujii, Y., Watanabe, O., and Vimeux, F.: Dome Fuji ice core preliminary temperature reconstruction, 0–340 kyr, ICBP PAGES/World Data Center for Paleoclimatology data contribution series 2007-074, NOAA, Boulder CO, USA, 2007. 3586

Lenaerts, J., van den Broeke, M., van de Berg, W., van Meijgaard, E., and Munneke, P. K.: A new, high-resolution surface mass balance map of Antarctica, Geophys. Res. Lett., submitted, 2010. 3585

Masson-Delmotte, V., Kageyama, M., Braconnot, P., Charbit, S., Krinner, G., Ritz, C., Guilyardi, E., Jouzel, J., Abe-Ouchi, A., Crucifix, M., Gladstone, R., Hewitt, C., Kitoh, A., LeGrande, A., Marti, O., Merkel, U., Motoi, T., Ohgaito, R., Otto-Bliesner, B., Peltier, W., Ross, I., Valdes, P., Vettoretti, G., Weber, S., Wolk, F., and Yu, Y.: Past and future polar amplification of climate change: climate model intercomparisons and ice-core constraints, Clim. Dynam., 26, 513–529, doi:10.1007/s00382-005-0081-9, 2006. 3585, 3592

Peltier, W.: Global glacial isostasy and the surface of the ice-age Earth: The ICE-5G (VM2) Model and GRACE, Ann. Rev. Earth Planet. Sc., 32, 111–149, doi:10.1146/annurev.earth.32.082503.144359, 2004. 3585

Petit, J., Jouzel, J., Raynaud, D., Barkov, N., Barnola, J., Basile, I., Bender, M., Chappellaz, J., Davis, J., Delaygue, G., Delmotte, M., Kotlyakov, V., Legrand, M., Lipenkov, V., Lorius, C., Pépin, L., Ritz, C., Saltzman, E., and Stievenard, M.: Climate and atmospheric history of the past 420,000 years from the Vostok ice core, Antarctica, Nature, 399, 429–436, 1999. 3586

Pollard, D. and DeConto, R.: Modeling West Antarctic ice sheet growth and collapse through the past five million years, Nature, 458, 329–332, doi:10.1038/nature07809, 2009. 3584

Rojas, M., Moreno, P., Kageyama, M., Crucifix, M., Hewitt, C., Abe-Ouchi, A., Ohgaito, R., Brady, E., and Hope, P.: The Southern Westerlies during the last glacial maximum in PMIP2 simulations, Clim. Dynam., 32, 525–548, doi:10.1007/s00382-008-0421-7, 2009. 3592

Steig, E., Morse, D., Waddington, E., Stuiver, M., Grootes, P., Mayewski, P., Twickler, M., and Whitlow, S.: Wisconsinan and Holocene climate history from an ice core at Taylor Dome, western Ross Embayment, Antarctica, Geogr. Ann. A, 82, 213–235, 2000. 3586

Stenni, B., Masson-Delmotte, V., Selmo, E., Oerter, H., Meyer, H., Röthlisberger, R., Jouzel, J., Cattani, O., Falourd, S., Fischer, H., Hoffmann, G., Iacumin, P., Johnsen, S., Minster, B., and Udisti, R.: The deuterium excess records of EPICA Dome C and Dronning Maud Land ice cores (East Antarctica), Quaternary Sci. Rev., 29, 146–159, doi:10.1016/j.quascirev.2009.10.009, 2010. 3586

Thomas, R.: The dynamics of marine ice sheets, J. Glaciol., 24, 167–177, 1979. 3584

van de Berg, W., van den Broeke, M., Reijmer, C., and van Meijgaard, E.: Characteristics of the Antarctic surface mass balance (1958–2002) using a regional atmospheric climate model, Ann. Glaciol., 41, 97–104, 2005. 3585

van Ommen, T., Morgan, V., and Curran, M.: Deglacial and Holocene changes in accumulation at Law Dome, East Antarctica, Ann. Glaciol., 39, 359–365, 2004. 3586, 3591

Yanase, W. and Abe-Ouchi, A.: The LGM surface climate and atmospheric circulation over East Asia and the North Pacific in the PMIP2 coupled model simulations, Clim. Past, 3, 439–451, doi:10.5194/cp-3-439-2007, 2007. 3585

Table 1. The models evaluated in this comparison study, with the abbreviations used in this paper, the horizontal resolution of their data and the length of the period used to determine the climatological mean. An X indicates whether the model provided output for 6 ka and/or 21 ka.

Model name in PMIP2 database	Abbreviation	Resolution lon × lat	Averaging time (yr)	6 ka	21 ka
CCSM	CCSM	2.81° × 2.81°	100	X	X
CNRM-CM33	CNRM	2.81° × 2.81°	300		X
CSIRO-Mk3L-1.0	CSIRO-1.0	5.63° × 3.22°	100	X	
CSIRO-Mk3L-1.1	CSIRO-1.1	5.63° × 3.22°	50	X	
ECBILTCLIO	Ecbiltclio	5.63° × 5.63°	50		X
ECBILTCLIOVE-CODE	Ecbiltcliove	5.63° × 5.63°	100	X	
ECHAM5-MPIOM1	ECHAM5	3.75° × 3.75°	50	X	
ECHAM53-MPIOM127-LPJ	ECHAM53	3.75° × 3.75°	3	X	X
FGOALS-1.0g	FGOALS	2.81° × 3°	100	X	X
FOAM	FOAM	7.5° × 4.5°	100	X	
GISSmodelE	GISS	5° × 3.92°	50	X	
HadCM3M2	HadCM3	3.75° × 2.5°	20		X
IPSL-CM4-V1-MR	IPSL	3.75° × 2.5°	100	X	X
MIROC 3.2	MIROC 3.2	2.81° × 2.81°	50	X	X
MIROC 3.2.2	MIROC 3.2.2	2.81° × 2.81°	100		X
MRI-CGCM2.3.4fa	MRI-fa	2.81° × 2.81°	100	X	
MRI-CGCM2.3.4nfa	MRI-nfa	2.81° × 2.81°	100	X	
UBRIS-HadCM3M2	UBRIS	3.75° × 2.5°	100	X	

Title Page
Abstract Introduction
Conclusions References
Tables Figures
◀| |▶
◀ ▶
Back Close
Full Screen / Esc
Printer-friendly Version
Interactive Discussion

Table 2. Observed (upper line) and modelled temperature differences in Kelvin between the MH and the present at three ice core locations. Modelled temperature differences are calculated by interpolating the four closest model data points.

	EDC	EDML	Fuji	Law	Vostok
Ice core	−0.4	0.5	−0.4	0.1	0.4
CCSM	0.1	0.0	0.1	0.1	0.3
CSIRO-1.0	0.4	0.3	0.4	0.3	0.4
CSIRO-1.1	0.4	0.9	0.2	0.4	0.4
Ecbiltcliove	0.3	0.3	0.1	0.3	0.1
ECHAM5	0.2	0.5	1.0	0.6	0.5
ECHAM53	0.4	0.0	0.4	0.3	0.5
FGOALS	0.1	0.3	0.5	0.3	0.2
FOAM	0.5	0.8	0.6	1.0	0.7
GISS	−0.3	−0.5	−0.2	−0.1	−0.2
IPSL	0.6	0.5	0.5	0.6	0.4
MIROC 3.2	0.2	0.2	0.3	0.2	0.2
MRI-fa	0.7	0.6	0.5	2.4	0.4
MRI-nfa	−0.5	−0.2	−0.2	−1.0	−0.2
UBRIS	0.7	0.7	0.7	0.7	0.9

Table 3. Observed (upper line) and modelled differences between 6 ka and present precipitation and the ratios of the 6 ka to the present precipitation at three ice core locations.

	Law		Talos		Vostok	
	difference ($\mathrm{mm\,yr^{-1}}$)	ratio	difference ($\mathrm{mm\,yr^{-1}}$)	ratio	difference ($\mathrm{mm\,yr^{-1}}$)	ratio
Ice core	0.0	1.00	13.5	1.21	0.5	1.03
CCSM	−6.2	0.98	−1.8	0.99	0.0	1.00
CSIRO-1.0	9.3	1.02	10.3	1.04	0.3	1.02
CSIRO-1.1	27.9	1.06	19.2	1.09	1.0	1.06
Ecbiltcliove	−7.75	0.98	−20.2	0.94	3.4	1.01
ECHAM5	−392.1	0.54	−201.2	0.51	−32.2	0.49
ECHAM53	20.1	1.04	5.6	1.02	0.2	1.01
FGOALS	−0.8	1.00	27.2	1.05	0.8	1.01
FOAM	22.3	1.05	2.3	1.01	0.8	1.03
GISS	−15.4	0.98	14.4	1.03	−1.3	0.95
IPSL	39.8	1.06	13.7	1.05	1.0	1.06
MIROC 3.2	31.8	1.05	3.5	1.01	−0.3	0.99
MRI-fa	11.8	1.02	−3.0	0.99	−0.4	1.00
MRI-nfa	−29.4	0.96	0.7	1.00	5.8	1.03
UBRIS	78.8	1.16	13.8	1.12	1.9	1.10

Table 4. Observed (upper line) and modelled temperature differences in Kelvin between the LGM and the present at five ice core locations.

	EDC	EDML	Fuji	Law	Taylor	Vostok
Ice core	−9.3	−7.4	−7.6	−2.9	−3.0	−8.1
CCSM	−10.3	−7.2	−9.4	−9.1	−8.8	−10.9
CNRM	−4.1	−6.4	−3.8	−1.2	−1.7	−5.5
Ecbiltclio	−3.8	−5.1	−4.3	−6.8	−6.0	−2.8
ECHAM53	−11.9	−7.0	−10.9	−6.5	−9.1	−11.6
FGOALS	−11.6	−12.4	−12.6	−11.2	−11.1	−12.9
HadCM3	−9.0	−6.4	−7.9	−4.1	−5.8	−10.3
IPSL	−5.3	−3.8	−5.3	−2.4	−5.1	−6.9
MIROC 3.2	−6.3	−4.9	−6.2	−3.9	−6.3	−6.7
MIROC 3.2.2	−8.4	−6.5	−7.9	−5.0	−9.2	−7.9

Table 5. Observed (upper line) and modelled differences between LGM and present precipitation and the ratios of the LGM to the present precipitation at three ice core locations.

	Law		Talos		Vostok	
	difference ($\mathrm{mm\,yr^{-1}}$)	ratio	difference ($\mathrm{mm\,yr^{-1}}$)	ratio	difference ($\mathrm{mm\,yr^{-1}}$)	ratio
Ice core	−584	0.07	−45.0	0.41	−9.0	0.55
CCSM	−124.6	0.56	−101.6	0.48	−19.5	0.27
CNRM	−89.9	0.83	8.2	1.03	−6.6	0.80
Ecbiltclio	−24.9	0.94	−169.1	0.60	−105.6	0.48
ECHAM53	−140.5	0.71	−103.5	0.58	−22.5	0.30
FGOALS	−865.1	0.43	−205.5	0.64	−39.4	0.35
HadCM3	−161.0	0.68	−36.0	0.71	−14.9	0.38
IPSL	37.3	1.06	−6.7	0.98	−9.1	0.49
MIROC 3.2	−100.4	0.84	−38.3	0.85	−12.8	0.49
MIROC 3.2.2	−142.6	0.72	−68.7	0.69	−12.0	0.45

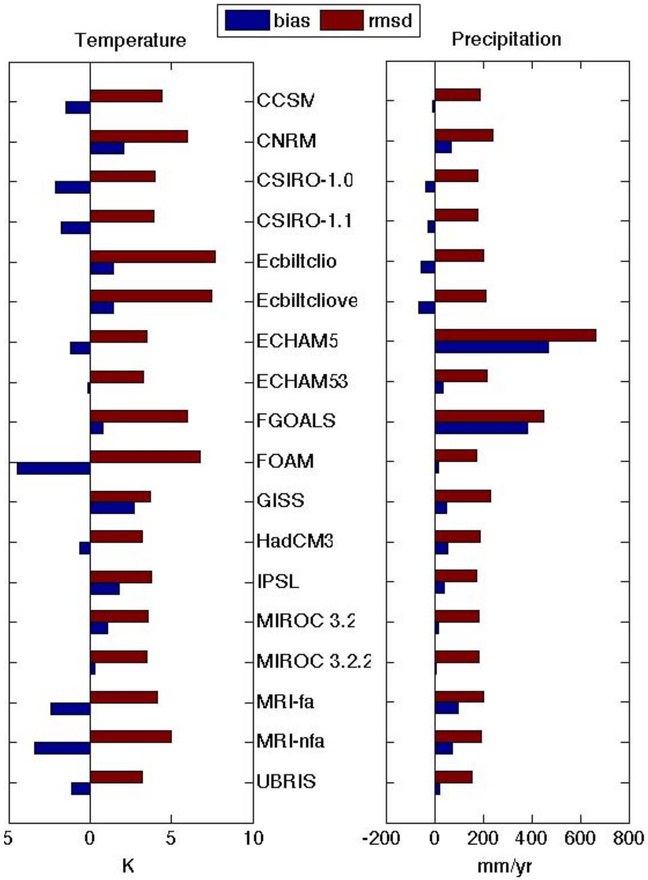

Fig. 1. The bias (in blue) and rmsd values (in red) for temperature (left panel) and precipitation (right panel) for all PMIP2 models as compared to the RACMO reference state, over the entire (RACMO) domain, for the present-day climate.

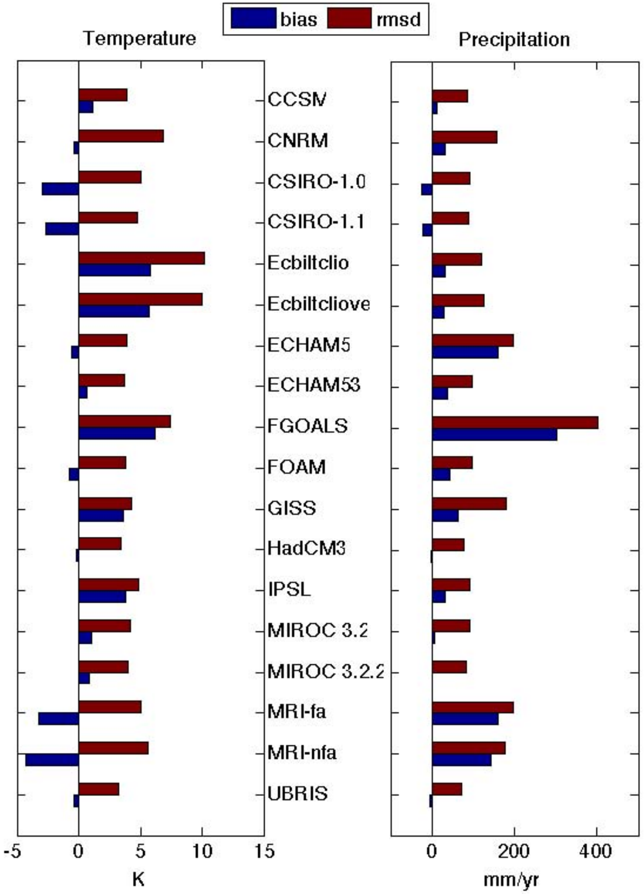

Fig. 2. The bias (in blue) and rmsd values (in red) for temperature (left panel) and precipitation (right panel) for all PMIP2 models as compared to the RACMO reference state, solely over the ice sheet, for the present-day climate.

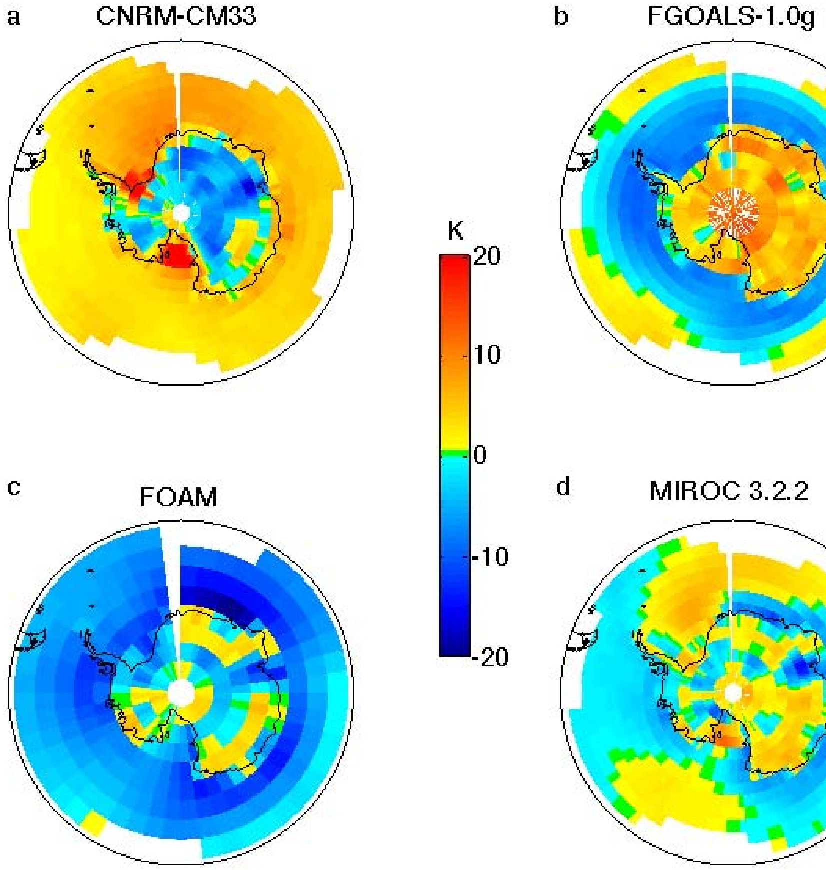

Fig. 3. Temperature difference fields between RACMO and **(a)** CNRM, **(b)** FGOALS, **(c)** FOAM and **(d)** MIROC 3.2.2.

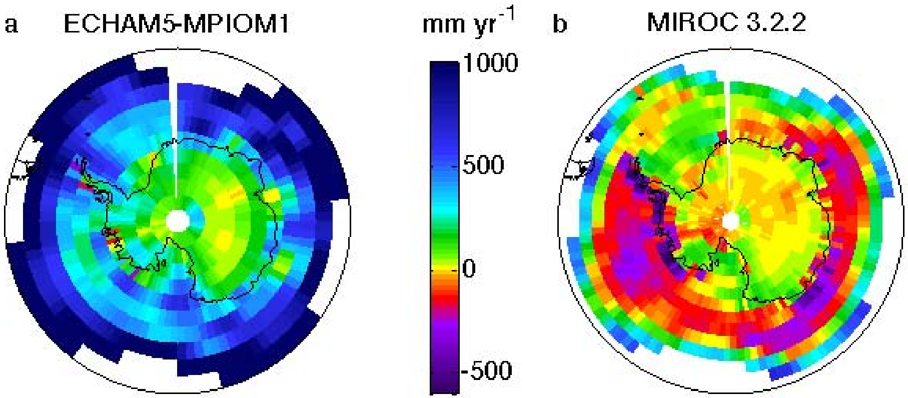

Fig. 4. Precipitation difference fields between RACMO and **(a)** ECHAM5, **(b)** MIROC 3.2.2.

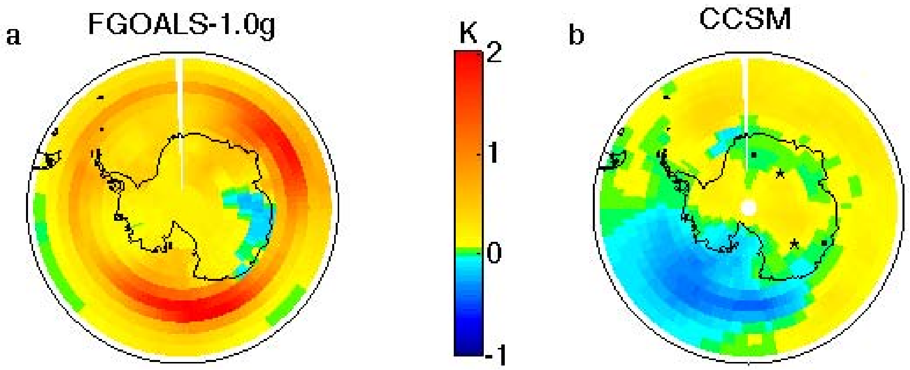

Fig. 5. Temperature difference fields between 6 ka and present-day GCM-output for **(a)** FGOALS and **(b)** CCSM. The squares indicate the locations of the EDML and Law Dome ice cores, the stars those of the Fuji and EDC ice cores.

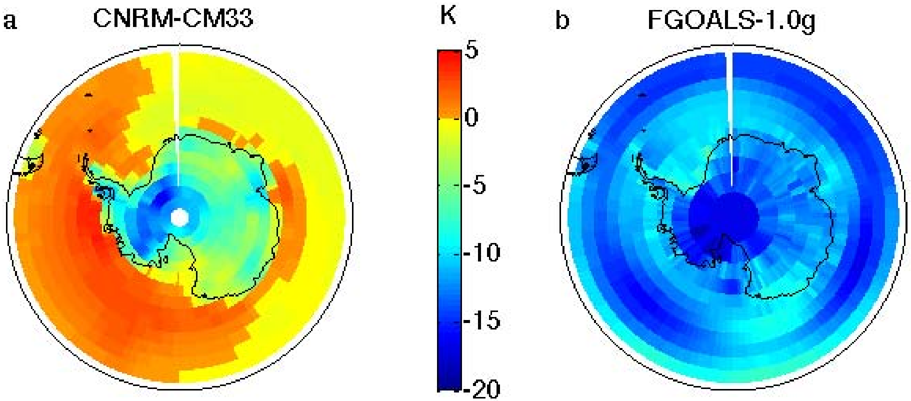

Fig. 6. Temperature difference fields between the LGM and present-day GCM-output for **(a)** CNRM and **(b)** FGOALS.

Title Page
Abstract
Introduction
Conclusions
References
Tables
Figures
◀|
|▶
◀
▶
Back
Close
Full Screen / Esc
Printer-friendly Version
Interactive Discussion

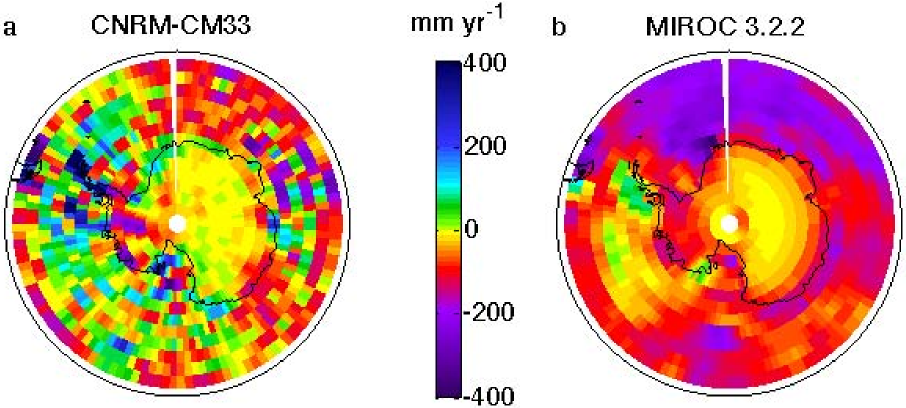

Fig. 7. Precipitation difference fields between the LGM and present-day GCM-output for **(a)** CNRM and **(b)** MIROC 3.2.2.